

# Congo red dye removal from aqueous solution by acid-activated bentonite from sarolangun: kinetic, equilibrium, and thermodynamic studies

*by Dedi Rohendi*

---

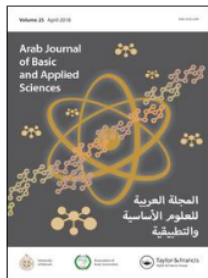
**Submission date:** 06-Oct-2022 09:08PM (UTC+0700)

**Submission ID:** 1918238308

**File name:** rom\_sarolangun\_kinetic\_equilibrium\_and\_thermodynamic\_studies.pdf (1.82M)

**Word count:** 7364

**Character count:** 38781



## Congo red dye removal from aqueous solution by acid-activated bentonite from sarolangun: kinetic, equilibrium, and thermodynamic studies

Tarmizi Taher, Dedi Rohendi, Risfidian Mohadi & Aldes Lesbani

To cite this article: Tarmizi Taher, Dedi Rohendi, Risfidian Mohadi & Aldes Lesbani (2019) Congo red dye removal from aqueous solution by acid-activated bentonite from sarolangun: kinetic, equilibrium, and thermodynamic studies, Arab Journal of Basic and Applied Sciences, 26:1, 125-136, DOI: [10.1080/25765299.2019.1576274](https://doi.org/10.1080/25765299.2019.1576274)

To link to this article: <https://doi.org/10.1080/25765299.2019.1576274>



© 2019 The Author(s). Published by Informa UK Limited, trading as Taylor & Francis Group on behalf of the University of Bahrain



Published online: 13 Apr 2019.



[Submit your article to this journal](#)



Article views: 27



[View Crossmark data](#)



## Congo red dye removal from aqueous solution by acid-activated bentonite from sarolangun: kinetic, equilibrium, and thermodynamic studies

Tarmizi Taher<sup>a</sup>, Dedi Rohendi<sup>b</sup>, Risfidian Mohadi<sup>b</sup> and Aldes Lesbani<sup>a,b</sup>

<sup>a</sup>Department of Environmental Sciences, Graduate School of Sriwijaya University, South Sumatra, Indonesia; <sup>b</sup>Department of Chemistry, Faculty of Mathematics and Natural Sciences, Sriwijaya University, South Sumatra, Indonesia

4

### ABSTRACT

The abundant natural bentonite from Sarolangun deposit of Jambi Province, Indonesia, has been successfully activated by a wet acid activation method and applied as a low-cost, and environmental-friendly adsorbent for Congo red dye removal from aqueous solution. The activated bentonite samples were characterized by powder X-ray diffraction (XRD), Fourier-transform infrared spectroscopy (FTIR), N<sub>2</sub> adsorption-desorption, and X-ray fluorescence (XRF). The batch adsorption technique has been conducted to study the adsorption behavior of Congo red on activated bentonite. The effects of operational parameters toward the Congo red adsorption on activated bentonite, including adsorbent dosage, initial pH, contact time, initial concentration, and temperature were investigated. Moreover, the properties of adsorption kinetics, adsorption isotherm, and adsorption thermodynamic were also investigated. The results of material characterization showed that acid-activated bentonite has better properties than natural bentonite. For instance, the surface area of acid-activated bentonite elevated almost five-fold compared with natural bentonite. The batch adsorption study showed that the Congo red adsorption on acid-activated bentonite was significantly affected by adsorbent dosage, initial pH, contact time, dye concentration, and temperature. The adsorption kinetics investigation revealed that adsorption was best evaluated by a pseudo-second-order model rather than pseudo-first-order model. The adsorption equilibrium study described that the adsorption process followed the Langmuir isotherm model. The result of thermodynamic investigation revealed that the adsorption process occurred spontaneously and favorably in high-temperature conditions.

### ARTICLE HISTORY

Received 15 October 2017  
Accepted 18 January 2019

### KEYWORDS

Natural bentonite; acid activation; adsorption; Congo red

## 1. Introduction

As one of many developing countries, growth of the traditional textile industry in Indonesia gradually increased year by year. During the dyeing process in the conventional textile industry, an amount of dye remain which can permeate the fabric and be released to the environment owing to limitations of the wastewater treatment plant (Irmanto & Suyata, 2008). Commonly, dyes used in the textile industry are synthetic with high resistance to oxidizing agents, biodegradation and photodegradation treatment (Wasti & Ali Awan, 2016). Based on the paper reported by Shu et al. (2015), Congo red is one of the most common synthetic dyes used in the textile industry. It is a group of benzidine-based anionic diazo dyes with high toxicity and irritant properties to eye and skin contact. At a high level of contamination, it could induce some respiratory problems and even could be a carcinogenic agent to humans. Consequently, Congo red removal from wastewater

of the textile industry is a necessity in order to avoid environmental issues.

In order to remove the dye contamination from wastewater, various technologies have been developed including filtration, coagulation, electrochemical oxidation, chemical oxidation, membrane filtration, adsorption or biosorption, and microbiological treatment (El Haddad, Regti, Slimani, & Lazar, 2014b; Peng, Luan, Chen, Tian, & Jia, 2005; Wang et al., 2016). Among all techniques mentioned, adsorption is considered as the most feasible method to remove the dye contamination in aqueous conditions (El Haddad, Mamouni, Saffaj, & Lazar, 2012). Adsorption is a well-known separation method with high effectivity for water contaminant removal. The adsorption technique currently appears as the most efficient method due to the simplest operation, adsorbent reuse capability, insensitivity to the toxic pollutant, high efficiency and, moreover, low-cost operation (Rafatullah, Sulaiman, Hashim, & Ahmad, 2010).

**CONTACT** Aldes Lesbani [aldeslesbani@pps.unsri.ac.id](mailto:aldeslesbani@pps.unsri.ac.id) Department of Environmental Sciences, Graduate School of Sriwijaya University, Jl. Padang Selasa, No. 524, Bukit Besar, Palembang 30139, South Sumatra, Indonesia

© 2019 The Author(s). Published by Informa UK Limited, trading as Taylor & Francis Group on behalf of the University of Bahrain. This is an Open Access article distributed under the terms of the Creative Commons Attribution License (<http://creativecommons.org/licenses/by/4.0/>), which permits unrestricted use, distribution, and reproduction in any medium, provided the original work is properly cited.

Recently, clay and clays mineral have been widely used in broad application fields, i.e. cosmetics, oil mining, pharmaceutical, food, and paper industries. The high demand on the clay's utilization in diverse areas is influenced by its natural abundance, low cost, high cation exchange capacity (CEC), large surface area, and high adsorption capacity. However, natural clays cannot be used as found and need further appropriate modification by chemical or physical methods (Bilgiç et al., 2014).

Bentonite is one of the most utilized clay materials. It is a naturally occurring clay that is mainly constituted of montmorillonite mineral. Bentonite is also well known as dioctahedral 2:1 layer silicate with high swelling properties. The substitution of  $Mg^{2+}$  for  $Al^{3+}$  in the octahedral structure and  $Al^{3+}$  for  $Si^{4+}$  in tetrahedral structure causes a permanent negative charge on the bentonite surface. This negative charge commonly equilibrates with the presence of exchangeable inorganic metal cations such as  $Ca^{+}$ ,  $Na^{+}$ , and  $Mg^{2+}$  located in the interlamellar space (Parolo, Pettinari, Musso, Sánchez-Izquierdo, & Fernández, 2014).

Today, many methods have been studied to increase the adsorption capacity of natural bentonite for contaminant removal from wastewater. Commonly, the clay materials can be modified by both physical and chemical treatment. Bentonite modification by thermal activation has increased the nature of bentonite as an adsorbent for dyes and heavy metals removal from aqueous solution. Thermally activated bentonite has been proved to be a highly efficient adsorbent for Congo red removal from wastewater (Toor, Jin, Dai, & Vimonses, 2015). Bentonite modification by chemical treatment has been widely developed, as reported in many publications (D'Amico, Ollier, Alvarez, Schroeder, & Cyras, 2014; Jing, Hou, Zhao, Tang, & Wan, 2013; Marsal, Bautista, Ribosa, Pons, & García, 2009; Mishra & Mahato, 2016).

The term "acid activation" represents one of the chemical treatments used on bentonite to produce the partially dissolved bentonite. By treating the bentonite with inorganic acids, the inorganic cation lying in the interlayer structure of bentonite will be replaced with the monovalent hydrogen ion. This replacement also leaches out the ferric, ferrous, aluminium, and other trace cations, so the smectite layer of the bentonite will be altered, and the specific surface area and the porosity will be increased (Komadel, 2016). This method is the most common preliminary chemical modification of clay and clay minerals especially bentonite for use in both scientific and industrial purposes.

In this work, the abundant natural bentonite from Sarolangun district, Jambi Province, Indonesia was

prepared and activated by the acid-activation method using  $H_2SO_4$  as an acid agent in order to elevate its natural properties such as the surface area and adsorption capability. The objective of this work was to investigate the feasibility of the local bentonite from Sarolangun be treated by the acid-activation method and used as an adsorbent material for Congo red removal. The adsorption behavior and effect of the experimental parameter including the adsorbent amount, contact time, dye concentration, and adsorption temperature were also investigated.

## 2. Materials and methods

### 2.1. Chemicals and instrumentation

Bentonite used in this work was natural bentonite from the Sarolangun deposit in Jambi Province, Indonesia. Sulfuric acid ( $H_2SO_4$ ) as an acid activator agent for bentonite was purchased from Sigma Aldrich. It is analytical reagent grade and used as received without further treatment or purification. Congo red as artificial dye adsorbate was purchased from Merck and used without further treatment. The adsorbent characterization using XRD was conducted using X-Ray diffraction on a Rigaku Miniflex 600 instrument equipped with Ni-filtered  $CuK\alpha$  radiation with scanning speed  $5^\circ \text{ min}^{-1}$ . FTIR analysis was carried out by FT-IR, a Shimadzu Prestige-21 instrument using KBr disc with a wavenumber  $400\text{--}4000 \text{ cm}^{-1}$ . Nitrogen adsorption-desorption isotherm analysis was conducted with an ASAP Micromeritics 2020 surface area analyzer. X-ray fluorescence analysis was carried out with a analytical type Minipal 4. Congo red concentration after the adsorption process was measured using a double beam UV-Vis spectrophotometer instrument from EMCLab type EMC-61PC-UV.

### 2.2. Natural bentonite activation and characterization

The natural reddish bentonite obtained from Sarolangun deposit, Indonesia, was used as the source material in order to form adsorbent to remove the Congo red dye. Before acid activation, the natural bentonite first was washed using distilled water three times in order to remove the impurities. The wet cleaned bentonite was dried at 378 K for eight hours and mashed in a porcelain mortar to enable passage through a 100-mesh standard ASTM sieve. The resulting material was then labelled as natural Sarolangun bentonite (NSbent).

The acid-activated bentonite was prepared based on the work carried out by Önal and Sarikaya (2007), using the wet chemical method. Prior to the

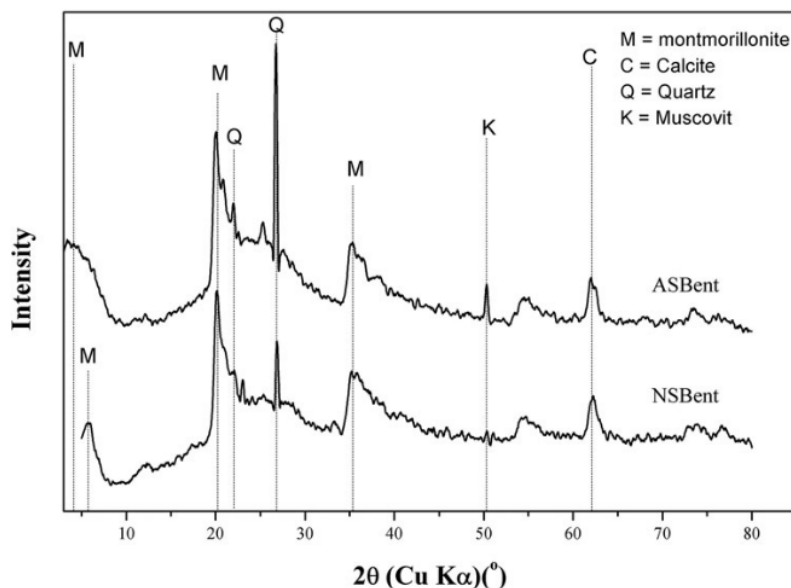


**Figure 1.** XRD patterns of natural Sarolangun bentonite (NSbent) and acid activated Sarolangun bentonite (ASbent) by various acid concentrations.

activation process, the NSbent samples were dried at 378 K for four hours, then 20 g of samples were mixed with 400 mL of H<sub>2</sub>SO<sub>4</sub> solution (10% by mass) for six hours at 363 K by stirring in a 1000 mL flask. After the acid treatment, the suspension was filtered and the precipitate washed using distilled water to remove the excess of SO<sub>4</sub><sup>2-</sup> ions. The acid treated NSbent was then dried at 378 K for eight hours and stored in a closed glass bottle. The acid-activated bentonite product was labelled as acid-activated "Sarolangun bentonite (ASbent)". Changes of bentonite properties before and after activation by H<sub>2</sub>SO<sub>4</sub> were investigated using X-ray diffraction (XRD), FT-IR, N<sub>2</sub> adsorption-desorption, and X-ray fluorescence.

### 2.3. Adsorption experiment

The adsorption of Congo red onto the ASbent was thoroughly examined using the batch adsorption system. Congo red stock solutions (1000 mg L<sup>-1</sup>) were prepared by dissolving 1 g Congo red powder in 1000 mL of distilled water. The working solution of Congo red was made by diluting the stock solution in the desired concentration with distilled water. Typically, 0.05 g of ASbent was added into a 100-mL conical flask containing 50 mL of Congo red solution of the predetermined concentration. The mixture was then stirred at 400 rpm at room temperature for a predetermined contact time. After this process, the mixture was separated using a centrifuge at 4000 rpm for five minutes. The remaining Congo red concentration was then determined using

a spectrophotometer. The percent removal and the adsorption capacity of the adsorption process were calculated by equation (1) and (2), respectively.

$$\% \text{removal} = \frac{C_0 - C_t}{C_0} \times 100 \quad (1)$$

$$q_t = \frac{(C_0 - C_t)V}{m} \quad (2)$$

where  $C_0$ ,  $C_t$ ,  $q_t$ ,  $V$ , and  $m$  are the initial Congo red concentration (mg L<sup>-1</sup>), Congo red concentration after desired contact time  $t$  (mg L<sup>-1</sup>), adsorption capacity (mg g<sup>-1</sup>), volume of the Congo red solution (L), and the amount of adsorbent used (g), respectively.

## 3. Results and discussion

### 3.1. Adsorbent characterization

The natural bentonite from Sarolangun (NSbent) was activated by sulfuric acid as a facile activation method. The NSbent and acid-activated bentonite from the Sarolangun (ASbent) samples had been subjected to powder X-ray diffraction analysis in order to study the change of the bentonite structure resulting from the activation process. The X-ray diffraction pattern for both NSbent and ASbent are presented in Figure 1. The result of the XRD analysis for NSbent showed that the used natural bentonite consists of montmorillonite, calcite, quartz, and muscovite minerals. The XRD pattern of the NSbent sample revealed the presence of the  $d_{001}$  reflection of the

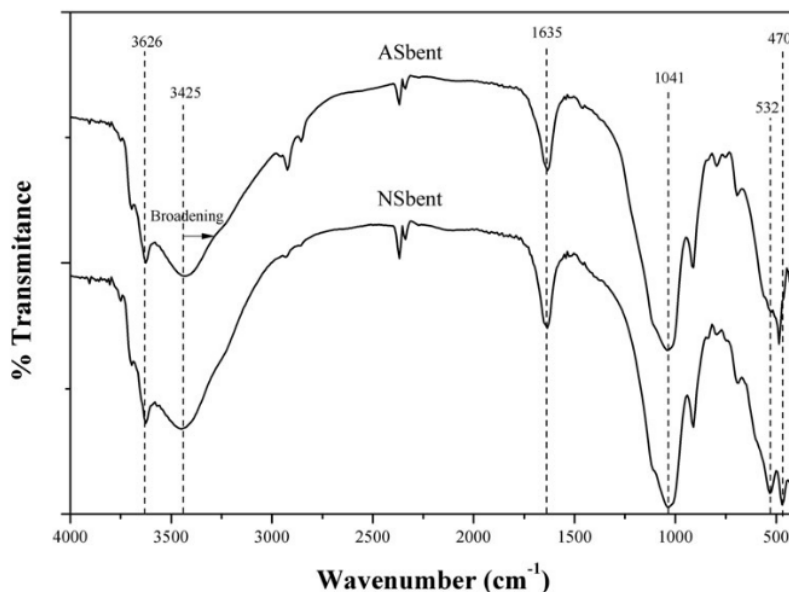


**Figure 2.** FTIR spectra of natural Sarolangun bentonite (NSbent), and activated Sarolangun bentonite (ASbent).

bentonite interlayer, which is present in  $2\theta$  about  $5.72^\circ$  with the basal spacing value of 1.51 nm. The presence of  $d_{100}$  reflection of the montmorillonite interlayer appeared at  $2\theta$  around  $20^\circ$ . The sharp reflection pattern emerged in the  $2\theta$  about  $27^\circ$  revealed the presence of quartz as impurities (Faghihian & Mohammadi, 2013).

After the acid activation, the XRD pattern of ASbent showed the broadening of the  $d_{001}$  reflection indicating that the layered structure of NSbent was partially destroyed due to acid activation, and also the crystallinity of the ASbent was affected (Pawar, Bajaj, & Lee, 2016). Moreover, the XRD pattern showed that after the acid activation, the  $2\theta$  reflection at  $5.72^\circ$  was shifted left to  $4.16^\circ$  (basal spacing increased from 1.51 to 1.99 nm). This phenomenon revealed a significant collapse of the crystalline structure. The increase of the quartz (Q) reflected at  $2\theta$  around  $27^\circ$  after the acid activation process showed that quartz as impurities was not destroyed in the process and the intensity was increased due to the smectite structure of the bentonite being partially destroyed.

In order to investigate the change in bentonite structure after the acid activation, FTIR spectroscopy was conducted due to its high sensitivity to the modification of the clay structure. During the acid activation, the proton from the acid penetrated into the bentonite layers and attached the OH group. As the dihydroxylation and partial dissolution of the smectite structure occurred, the changes in the characteristics of the absorption bands of the OH vibration will be recorded in IR spectra. The FTIR spectra

NSbent and ASbent are shown in Figure 2. The characteristic vibration peaks of the NSbent were recorded at wavenumber 470, 532, 910, 1041, 1635, 3425, and  $3626\text{ cm}^{-1}$  (Pawar et al., 2016). The two adjacent vibration peaks observed at 3425 and  $3626\text{ cm}^{-1}$  were attributed to the stretching vibration band of the OH section of the hydroxyl group on the bentonite structure and the water molecules present in the interlayer space (Tomul, 2011). The band observed at the wavenumber  $1635\text{ cm}^{-1}$  was also attributed as the OH deformation vibration from the water molecule (Kumararaja, Manjaiah, Datta, & Sarkar, 2017). After the acid activation, as can be seen in Figure 2, the band at  $3425\text{ cm}^{-1}$  which was broadened as the effect of the introduction of the -OH group due to the partial dissolution of the main bentonite structure.

The sharp vibration band at wavenumber  $1041\text{ cm}^{-1}$  is reported as the stretching vibration of Si-O group (He et al., 2012). Due to the dissolution during the acid activation, the band of the Si-O group decreased. The NSbent spectra showed the specific vibration band of the Al-O-Si group recorded at wavenumber 532 and  $470\text{ cm}^{-1}$  as the stretching and bending vibration band (Kumararaja et al., 2017), while for the ASbent spectra, the vibration band at  $530\text{ cm}^{-1}$  was not observed and the band at  $470\text{ cm}^{-1}$  was shifted to  $486\text{ cm}^{-1}$ . As reported by Özcan and Özcan (2004), this phenomenon is an indication that the layers structure remains after the activation process.

The  $\text{N}_2$  adsorption-desorption analysis has been subjected to the NSbent and ASbent samples to

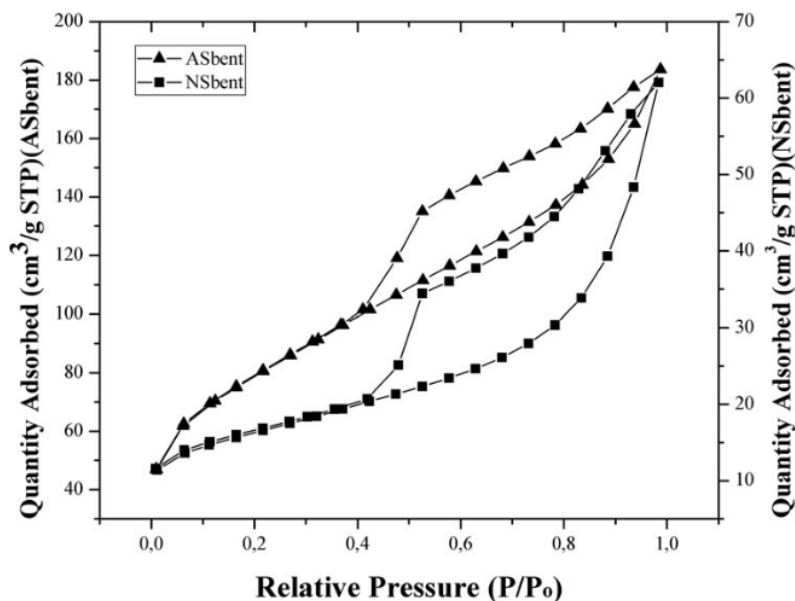


Figure 3. N<sub>2</sub> Adsorption-desorption isotherm of NSbent and ASbent.

investigate the change of the textural properties during the acid activation process. The N<sub>2</sub> adsorption-desorption isotherm for the NSbent and ASbent samples is presented in Figure 3. The results clearly illustrate that the isotherm pattern of these samples follows the type IV based on IUPAC adsorption isotherm classification. The further data of the NSbent and ASbent textural properties are shown in Table 1. The obtained data showed that the acid activation process has significantly elevated the surface properties of the natural bentonite. The ASbent has five-fold higher surface area than the NSbent. The pore volume of ASbent was also increased three-fold compared with the NSbent. The increasing quality of the textural properties after acid activation occurs because particles inside the dissolved octahedral sheets were split (Pawar et al., 2016).

The result of the XRF analysis of NSbent and ASbent samples are depicted in Figure 4. Both NSbent and ASbent are mainly constructed by Al<sub>2</sub>O<sub>3</sub> and SiO<sub>2</sub>, with the presence of trace elements of various metal oxides. The results clearly show that the acid activation process successfully changed the chemistry of the natural bentonite. After acid activation, the abundance of some metallic oxides particularly Fe<sub>2</sub>O<sub>3</sub>, TiO<sub>2</sub>, MnO, V<sub>2</sub>O<sub>5</sub>, NiO, CuO, and ZnO was reduced. This phenomenon indicates that these metal oxides, which correspond to the inorganic interlayer cation, were dissolved readily during the acid activation process, while the abundance of Al<sub>2</sub>O<sub>3</sub> was not changed and SiO<sub>2</sub> was significantly increased. This finding shows that the layered structure of the bentonite constructed by Al<sub>2</sub>O<sub>3</sub> and SiO<sub>2</sub>

Table 1. The textural properties of bentonite samples based on N<sub>2</sub> adsorption-desorption isotherm.

Properties	Samples	
	NSbent	ASbent
BET Surface Area (m <sup>2</sup> g <sup>-1</sup> )	55.8719	278.7961
Langmuir surface area (m <sup>2</sup> g <sup>-1</sup> )	231.9062	820.6051
BJH surface area (m <sup>2</sup> g <sup>-1</sup> )	39.546	209.795
Total Pore volume (cm <sup>3</sup> g <sup>-1</sup> )	0.0959	0.2841
Micropore volume (cm <sup>3</sup> g <sup>-1</sup> )	0.0069	0.0118
Average pore width (nm)	6.8710	4.0770
BJH pore diameter (nm)	8.7765	4.7021

provides much resistance to the acidic condition. The increase of the SiO<sub>2</sub> content was caused by the reduction of other cations that lie in the interlayer and octahedral sheets (Elfadly, Zeid, Yehia, Abouelela, & Rabie, 2017).

### 3.2. Effect of initial pH

As one of the diazo class dyes, the form of the Congo red molecule in the aqueous solution will be affected by the pH value. As mentioned by Lian, Guo, & Guo (2009), the color of Congo red changed significantly from red to dark blue when the pH of the solution was reduced to 2. On the other hand, when the pH of Congo red solution was adjusted to be more than 10, its color was different from the original. Hence, in this work, the effect of initial pH solution on the adsorption of Congo red on ASbent was studied at a pH ranging from 5 to 9 for an initial concentration of Congo red of 100 mg/L. Figure 5 shows the effect of initial pH of Congo red solution toward the adsorption capacity of ASbent. The results indicate that the adsorption of Congo red on

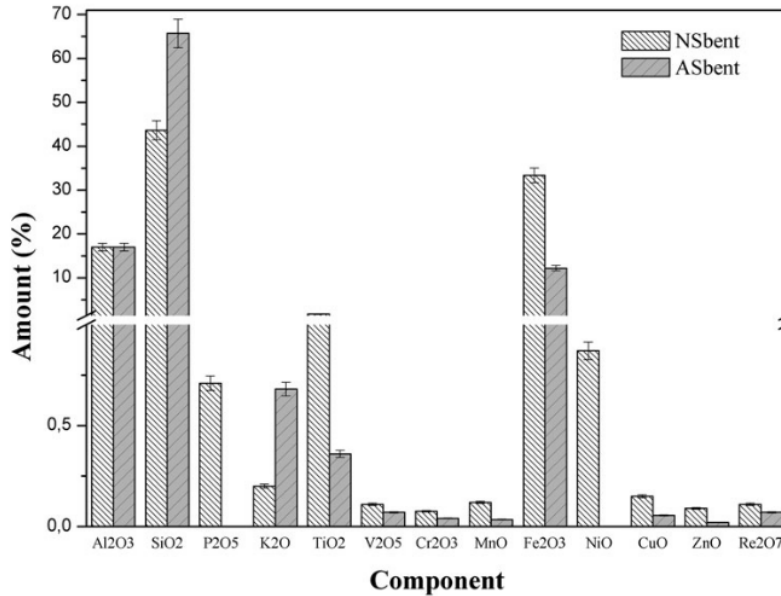


Figure 4. XRF analysis result for NSbent and ASbent samples.

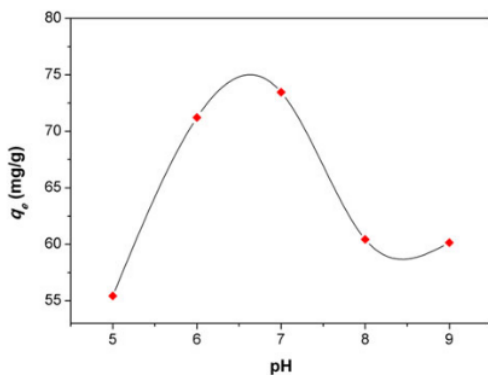


Figure 5. Effect of initial pH on the adsorption capacity ( $q_e$ ).

ASbent was profoundly affected by the pH of the solution. The most favored adsorption process occurred at a neutral pH (pH 6 to 7). By increasing the pH to be more than 7, the adsorption capacity decreased then remained relatively constant after pH 8. Moreover, below pH 6 (acidic condition), the adsorption capacity also decreased by decreasing the solution pH.

### 3.3. Effect of adsorbent dosage

The effect of the adsorbent amount on Congo red adsorption was tested by contacting various amounts of the adsorbent with 50 mL of 50 mg L<sup>-1</sup> Congo red solution at room temperature for 30 min. The result of the experiment in the form of a graph of the amount of adsorbent dosage against percent removal and adsorption capacity ( $q_e$ ) is presented in

Figure 6. The graph describes that by increasing the amount of adsorbent, the percent removal of Congo red on ASbent was also gradually increased, while for the adsorption capacity, the result showed that the maximum adsorption capacity was reached when the adsorbent dosage was in the range of 0.05 to 0.1 g. As the adsorbent amount increased, the number of active sites available during the adsorption increased as well, and thus the percentage of the removal also increased since all active sites may not be available during the adsorption due to the overlapping between the active sites themselves, and so the adsorbed amount of the adsorbent decreases.

### 3.4. Adsorption kinetic study

In this work, the adsorption kinetic study was conducted by several batch adsorption experiments at various contact times. 0.05 g of ASbent had contact with 50 mL of 50 mg L<sup>-1</sup> Congo red solution, which was then agitated using a magnetic stirrer for different contact time in the range of 0 to 60 min at room temperature. Figure 7 shows the effect of contact time on the adsorption capacity of the activated bentonite adsorbent. The graph indicates that the adsorption of the Congo red on activated bentonite rapidly occurred in the first 5 min' contact time and gradually slowed down after 10 min' contact time until the adsorption process attaining equilibrium state within 30 min.

Similar outcomes to these results were also reported in our previous work (TaHER, Mohadi,



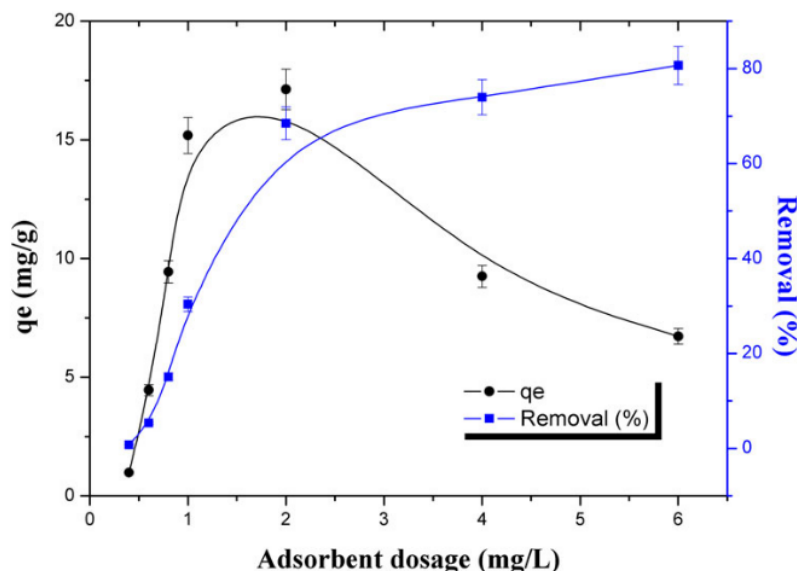


Figure 6. Effect of adsorbent dosage on the percent removal and adsorption capacity of Congo red onto ASbent adsorbent.

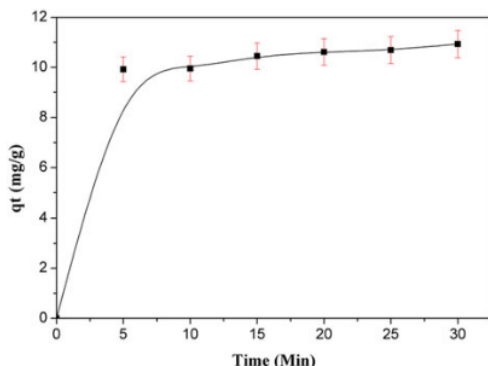


Figure 7. Effect of contact time on the adsorption capacity of Congo red onto activated bentonite.

Rohendi, & Lesbani, 2017) and many articles before that (Du et al., 2017; Goswami and Phukan, 2017; Rostami, Kaya, Gür, Onganer, & Meral, 2015). These indicated that, in the beginning, the Congo red molecules were adsorbed on the exterior surface of the activated bentonite adsorbent. The rapid adsorption during the first stage of adsorption was due to the most active site of the bentonite being unoccupied. After most of the adsorbent active sites had been occupied, the force between the Congo red as adsorbate with the adsorbent was gradually decreased and caused a reduction in the speed of adsorption. After the active exterior sites of the adsorbent had been entirely fulfilled, the adsorption process continues into the interior active sites of the adsorbent particles or into the interlayers of the bentonite; this process takes a relatively long time (Wang, Zheng, Deng, Feng, & Fu, 2013).

The adsorption rate constant and the adsorption mechanism of Congo red on ASbent was investigated based on the pseudo-first-order and pseudo-second-order kinetic model. The pseudo-first-order kinetic model was developed for the adsorption of solid/liquid system that suggested by Lagergren (Source). The equation for the pseudo-first-order kinetic model is described as follows:

$$dq/dt = k_1(q_e - q_t) \quad (3)$$

By integrating the equation with initial condition  $q_t = 0$  at  $t = 0$ , the equation can be transformed into a linear equation under boundaries conditions as follows:

$$\ln(q_e - q_t) = \ln q_e - k_1 t \quad (4)$$

$$\log(q_e - q_t) = \log q_e - \frac{k_1}{2.303} t \quad (5)$$

where  $q_e$  and  $q_t$  are the amount of Congo red adsorbed at equilibrium and at any time  $t$  ( $\text{mg g}^{-1}$ ), respectively. The pseudo-first-order kinetic rate constant is represented as  $k_1$ . The pseudo-first-order constant was measured by plotting the  $\log(q_e - q_t)$  against  $t$ .

The pseudo-second-order kinetic model was investigated based on the assumption that the adsorption experiments have been carried out in the equilibrium condition. The mathematical equation for the pseudo-second-order kinetic model is presented as follows:

$$\frac{dq_t}{dt} = k_2(q_e - q_t)^2 \quad (6)$$

The linear form of the equation can be presented by integrating the equation with the initial condition of  $q_t = 0$  at  $t = 0$  as follows:

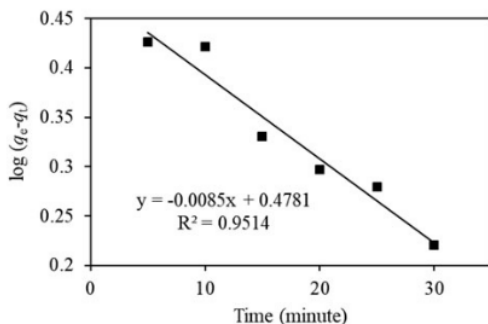


Figure 8. Plot Time versus  $\log(q_e - q_t)$ .

$$\frac{t}{q_t} = \frac{1}{k_2 q_e^2} + \frac{1}{q_e} t \quad (7)$$

where  $k_2$  is the pseudo-second-order rate constant,  $q_e$  and  $q_t$  are the amounts of Congo red adsorbed at equilibrium and at any time  $t$  ( $\text{mg g}^{-1}$ ), respectively.

The result for the pseudo-first-order and pseudo-second-order kinetic model of Congo red on ASbent is presented in Figures 8 and 9, respectively. The comparison of both figures describes that the coefficient correlation for the plot of the pseudo-second-order equation is higher than the pseudo-first-order kinetic model. The coefficient correlation ( $R^2$ ) value is 0.9514 for the pseudo-first-order kinetic model, and 0.9993 for the pseudo-second-order kinetic model. This finding reveals that the adsorption of Congo red on ASbent was better described based on the pseudo-second-order kinetic than the pseudo-first-order kinetic model. Since the pseudo-second-order kinetic model was based on the equilibrium capacity, this result also revealed that the adsorption rate of the Congo red on ASbent depends on the dye concentration at the ASbent surface at equilibrium (Wang & Wang, 2008). This finding also described that the rate determining step of Congo red adsorption on ASbent was a chemisorption (El Haddad et al., 2014b). The overall value of the kinetic study of Congo red on ASbent is presented in Table 2.

### 3.5. Adsorption equilibrium study

The design of the adsorbate adsorption can be optimized by looking up the most appropriate correlation of the equilibrium curve. The adsorption isotherm described the equilibrium between the adsorbate that was adsorbed onto the active site of the adsorbent and the adsorbate retained in the solution. Previously, many adsorption isotherm models have been developed such as Langmuir (1918), Freundlich (1907), Redlich and Peterson (1959), Temkin, Dubinin-Radushkevich. However, the most frequently used models were Langmuir and Freundlich models (Božić et al., 2013). Here, in this

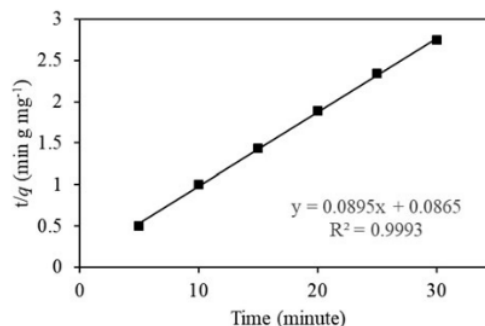


Figure 9. The plot times against  $t/q$ .

Table 2. Constant of kinetic models of Congo red removal by ASbent.

Kinetic Model	Parameters	Congo red
Pseudo-first-order	$q_e$ experimental ( $\text{mg g}^{-1}$ )	12.5
	$q_e$ calculated ( $\text{mg g}^{-1}$ )	3.0
	$k_1$ ( $\text{min}^{-1}$ )	0.0195
	$R^2$	0.9513
Pseudo-second-order	$q_e$ experimental ( $\text{mg g}^{-1}$ )	12.5
	$q_e$ calculated ( $\text{mg g}^{-1}$ )	11.1787
	$k_2$ ( $\text{g/mg min}$ )	0.0925
	$R^2$	0.9992

experimental work, the adsorption isotherm was studied based on these Langmuir and Freundlich models to explain the relation between dye adsorbed on the adsorbent and the concentration of the dye in the liquid phase (Wang, Pan, Cai, Guo, & Xiao, 2017).

The Langmuir isotherm model is the most widely used adsorption isotherm model applied for adsorption of any substance, in particular for pollutants removal from aqueous solutions. (Bulut, Özacar, & Şengil, 2008). The general Langmuir isotherm equation is presented in equation (8) as follows:

$$q_e = q_m \frac{K_L C_e}{1 + K_L C_e} \quad (8)$$

The linear form of the equation (8) is:

$$\frac{C_e}{q_e} = \frac{1}{K_L q_m} + \frac{C_e}{q_m} \quad (9)$$

where  $K_L$  and  $q_m$  are the Langmuir constant based on the adsorption energy ( $\text{L mg}^{-1}$ ) and the maximum amount of adsorption related to complete monolayer coverage on the surface of the adsorbent ( $\text{mg g}^{-1}$ ).

The prediction about the affinity between the adsorbate and the adsorbent (adsorption favorability) also can be predicted from the Langmuir parameter based on the dimensionless separation factor ( $R_L$ ) that is defined by equation 10 as follows:

$$R_L = \frac{1}{1 + K_L C_0} \quad (10)$$

where  $K_L$  and  $C_0$  are the Langmuir constant ( $\text{L g}^{-1}$ ) and initial concentration of Congo red as adsorbate

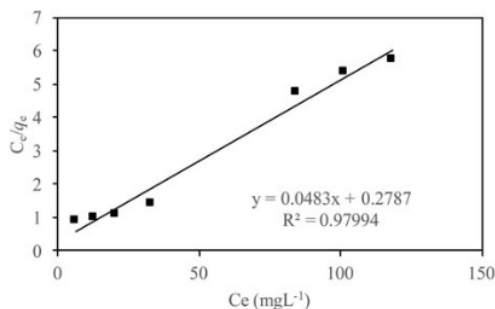


Figure 10. Plot  $C_e$  versus  $C_e/q_e$ .

( $\text{mg L}^{-1}$ ), respectively. The value of  $R_L$  was used to predict the isotherm type of the adsorption which occurred. If the  $R_L$  value is higher than 1 ( $R_L > 1$ ), it means that the adsorption is unfavorable. If the  $R_L$  value is less than 1 ( $R_L < 1$ ), it means that the adsorption process is linear. The adsorption is favorable if the  $R_L$  value is higher than zero and less than 1 ( $0 < R_L < 1$ ), and the adsorption is irreversible if the  $R_L$  value is equal to 0 ( $R_L = 0$ ) (El Haddad, Slimani, Mamouni, ElAntri, & Lazar, 2013; Xiyili, Çetintas, & Bingöl, 2017).

The Freundlich isotherm model is one of the adsorption isotherm models that can be used to predict the adsorption capacity of the adsorbent. The mathematical equation for the Freundlich isotherm model is presented as follows:

$$q_e = k_f C_e^{\frac{1}{n}} \quad (11)$$

The equation can be transformed into the linear form as follows:

$$\log q_e = \frac{1}{n} \log C_e + \log k_f \quad (12)$$

where  $k_f$  is the constant of the Freundlich model which corresponds to the adsorption capacity, and  $n$  is defined as the heterogeneity factor. Further, the  $n$  value can be used to predict the probability of the adsorption process, where with  $n > 1$  it means that the adsorption process was favorable. The useful value of  $k_f$  and  $n$  can be determined based on the intercept and slope of the linear plot of  $\log q_e$  against  $\log C_e$ .

The plot of the linear form for the Langmuir and Freundlich isotherm model is presented in Figures 10 and 11, respectively. Both figures show the coefficient correlation ( $R^2$ ) of the data conformi to the Langmuir and Freundlich isotherm model. The result showed that the Langmuir isotherm model was better described by Langmuir isotherm, which has higher  $R^2$  value (further confirmed in Figure 12). The  $R^2$  value for the Langmuir isotherm model is calculated as 0.9799, while the Freundlich model is 0.652. The whole adsorption kinetic parameter based on the Freundlich and Langmuir model is illustrated in Table 3.

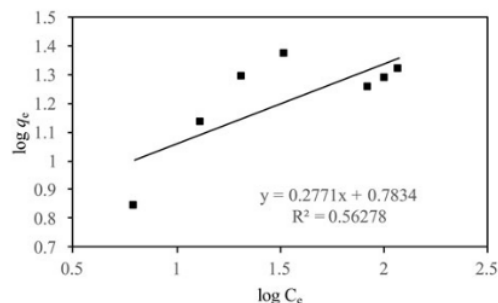


Figure 11. Plot  $\log C_e$  versus  $\log q_e$ .

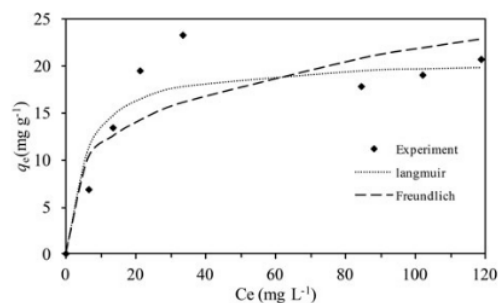


Figure 12. Adsorption isotherm of Congo red onto ASbent fitted by Langmuir and Freundlich model.

Table 3. The adsorption isotherm parameters for Congo red adsorption onto ASbent.

Langmuir Isotherm		Freundlich Isotherm				
$q_m$ ( $\text{mg g}^{-1}$ )	$K_L$ ( $\text{L mg}^{-1}$ )	$R_L$	$R^2$	$K_f$	$n$	$R^2$
20.7039	0.1794	0.0336–0.2179	0.9799	6.0729	3.6088	0.5627

### 3.6. Thermodynamic properties

Temperature is an important parameter of the thermodynamic adsorption properties. The effect of adsorption temperature toward the Congo red adsorption onto ASbent was investigated at various temperatures (303, 315, 323, and 333 K). The adsorption data were then used to determine the thermodynamic parameters of the adsorption process including the change of Gibb's free energy ( $\Delta G^0$ ), enthalpy ( $\Delta H^0$ ), and entropy ( $\Delta S^0$ ). The value of these three basic thermodynamic parameters was measured by the following equation:

$$\ln \left( \frac{q_e}{C_e} \right) = \frac{\Delta S^0}{R} - \frac{\Delta H^0}{RT} \quad (13)$$

$$\Delta G^0 = \Delta H^0 - T\Delta S^0 \quad (14)$$

where  $R$  is the gas constant ( $8.314 \text{ J mol}^{-1} \text{ K}^{-1}$ ), and  $T$  is the absolute temperature (K).

The value of the change of enthalpy ( $\Delta H^0$ ) and entropy ( $\Delta S^0$ ) was calculated as the slope and intercept of the linear plot  $\ln \left( \frac{q_e}{C_e} \right)$  versus  $1/T$ ,

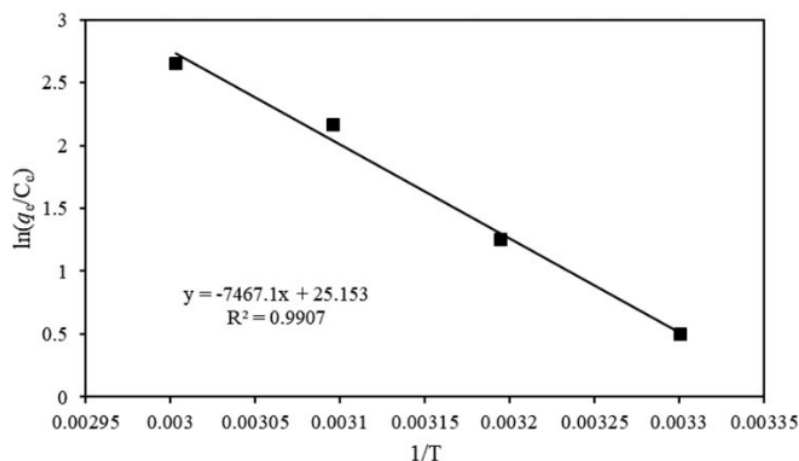


Figure 13. Plot of  $\ln(q_e/C_e)$  against  $1/T$  for Congo red adsorption onto ASbent.

Table 4. Thermodynamic parameters of Congo red adsorption onto ASbent.

$\Delta H^0$ (kJ/mol)	$\Delta S^0$ (J/mol K)	$\Delta G^0$ (kJ/mol)			
		303 K	313 K	323 K	333 K
62.081	209.122	-1.246	-3.336	-5.426	-7.516

respectively. As depicted in Figure 13, the coefficient correlation for the linear plot of  $\ln(q_e/C_e)$  against  $1/T$  was more than 0.98. It indicates that the linear equation obtained has good regression value. The values of the basic thermodynamic parameters are presented in Table 4.  $\Delta H^0$  and  $\Delta S^0$  values for Congo red adsorption onto activated bentonite were  $62.081 \text{ kJ mol}^{-1}$  and  $209.122 \text{ J mol}^{-1} \text{ K}^{-1}$ , respectively. The positive value for the change of the enthalpy ( $\Delta H^0$ ) indicates that the adsorption is undergoing the endothermic process. Also, the positive value of the change of entropy ( $\Delta S^0$ ) revealed that the during the adsorption process, the randomness of the solid-solution interface was increased (El Haddad et al., 2014a; Xiyili et al., 2017).

As shown in Table 4, the negative value of the  $\Delta G^0$  indicates that the Congo red adsorption onto ASbent is a spontaneous process (Slimani et al., 2014). Moreover, the result showed that by increasing the adsorption temperature, the  $\Delta G^0$  values gradually decreased. This phenomenon indicates that the adsorption process is more favorable at high temperatures. (Maleki, Hayati, Najafi, Gharibi, & Joo, 2016). Generally, the  $\Delta G^0$  value for physical adsorption is in the range of 0 to  $-20 \text{ kJ mol}^{-1}$ , while the  $\Delta G^0$  value for the chemical adsorption is in the range of  $-80$  to  $-400 \text{ kJ mol}^{-1}$  (Liu, Zheng, Wang, Jiang., & Li, 2010). The result of  $\Delta G^0$  value for the adsorption as described in Table 4 is in the range  $-1$  to  $-7 \text{ kJ mol}^{-1}$ . This result indicates that the Congo red adsorption onto activated bentonite follows the physical adsorption mechanism.

#### 4. Conclusion

Acid-activated bentonite prepared from natural bentonite Grounded from the Sarolangun deposit, Jambi Province, Indonesia was investigated in terms of its adsorption capability to remove Congo red from aqueous solution. The characterization of the natural bentonite sample before and after acid treatment showed that the structure of the natural bentonite was successfully modified. The maximum adsorption capacity of the ASbent based on the adsorption isotherm study was noted as  $20.7 \text{ mg g}^{-1}$ . The result of the adsorption kinetic study revealed that the pseudo-second-order kinetic model is more appropriate than the pseudo-first-order kinetic model. For the adsorption isotherm model, based on the experiment data, the Langmuir isotherm model is fit well to illustrate the adsorption isotherm of the Congo red onto ASbent.

#### Acknowledgements

The authors acknowledge the "Kementrian Riset, Teknologi, dan Pendidikan Tinggi (Kemenristekdikti) of Republic Indonesia, for financially supporting this research through Pendidikan Magister 13 tuju Doktor Untuk Sarjana Unggul (PMDSU) Batch II" research grant with contract number 468/UN9.3.1/LT/2017 and 326/SP2H/LT/DRPM/IX/2016.

#### 12 Disclosure statement

No potential conflict of interest was reported by the authors.

#### ORCID

Tarmizi Taher <http://orcid.org/0000-0002-3888-7730>  
Risfedian Mohadi <http://orcid.org/0000-0003-4974-4329>

## References

- Bilgiç, C., Topaloğlu Yazıcı, D., Karakehya, N., Çetinkaya, H., Singh, A., & Chehimi, M. M. (2014). Surface and interface physicochemical aspects of intercalated organo-bentonite. *International Journal of Adhesion and Adhesives*, 50, 204–210.
- Božić, D., Gorgievski, M., Stanković, V., Štrbac, N., Šerbula, S., & Petrović, N. (2013). Adsorption of heavy metal ions by beech sawdust – Kinetics, mechanism and equilibrium of the process. *Ecological Engineering*, 58, 202–206.
- Bulut, E., Özacar, M., & Şengil, İA. (2008). Equilibrium and kinetic data and process design for adsorption of Congo Red onto bentonite. *Journal of Hazardous Materials*, 154(1-3), 613–622. doi:10.1016/j.jhazmat.2007.10.071
- D'Amico, D. A., Ollier, R. P., Alvarez, V. A., Schroeder, W. F., & Cyras, V. P. (2014). Modification of bentonite by combination of reactions of acid-activation, silylation and ionic exchange. *Applied Clay Science*, 99, 254–260. doi:10.1016/j.clay.2014.07.002
- Du, S., Wang, L., Xue, N., Pei, M., Sui, W., & Guo, W. (2017). Polyethyleneimine modified bentonite for the adsorption of amino black 10B. *Journal of Solid State Chemistry*, 252, 152–157. doi:10.1016/j.jssc.2017.04.034
- El Haddad, M., Mamouni, R., Saffaj, N., & Lazar, S. (2012). Removal of a cationic dye - Basic Red 12 - from aqueous solution by adsorption onto animal bone meal. *Journal of the Association of Arab Universities for Basic and Applied Science*, 12, 48–54. doi:10.1016/j.jaubas.2012.04.003
- El Haddad, M., Regti, A., Laamari, M. R., Slimani, R., Mamouni, R., Antri, S. E., & Lazar, S. (2014a). Calcined mussel shells as a new and eco-friendly biosorbent to remove textile dyes from aqueous solutions. *Journal of the Taiwan Institute of Chemical Engineers*, 45(2), 533–540. doi:10.1016/j.jtice.2013.05.002
- El Haddad, M., Regti, A., Slimani, R., & Lazar, S. (2014b). Assessment of the biosorption kinetic and thermodynamic for the removal of safranin dye from aqueous solutions using calcined mussel shells. *Journal of Industrial and Engineering Chemistry*, 20(2), 717–724. doi:10.1016/j.jiec.2013.05.038
- El Haddad, M., Slimani, R., Mamouni, R., ElAntri, S., & Lazar, S. (2013). Removal of two textile dyes from aqueous solutions onto calcined bones. *Journal of the Association of Arab Universities for Basic and Applied Science*, 14, 51–59. doi:10.1016/j.jaubas.2013.03.002
- Elfadly, A. M., Zeid, I. F., Yehia, F. Z., Abouelela, M. M., & Rabie, A. M. (2017). Production of aromatic hydrocarbons from catalytic pyrolysis of lignin over acid-activated bentonite clay. *Fuel Processing Technol*, 163, 1–7. doi:10.1016/j.fuproc.2017.03.033
- Faghihian, H., & Mohammadi, M. H. (2013). Surface properties of pillared acid-activated bentonite as catalyst for selective production of linear alkylbenzene. *Applied Surface Science*, 264, 492–499. doi:10.1016/j.apsusc.2012.10.050
- Freundlich, H. (1907). Über die adsorption in Lösungen. *Zeitschrift für Physikalische Chemie* 57U, 385–470. doi:10.1515/zpch-1907-5723
- Goswami, M., & Phukan, P. (2017). Enhanced adsorption of cationic dyes using sulfonic acid modified activated carbon. *Journal of Environmental Chemical Engineering*, 5(4), 3508–3517. doi:10.1016/j.jece.2017.07.016
- He, S., Zhang, D., Gu, L., Zhang, S., & Yu, X. (2012). Bromate adsorption using Fe-pillared bentonite. *Environmental Technology*, 33(20), 2337–2344. doi:10.1080/09593330.2012.666571
- Irmanto, I., & Suyata, S. (2008). Penurunan BOD dan COD limbah cair industri tekstil di Kabupaten Pekalongan dengan metode multi soil layering. *Molekul*, 3(2), 98. doi:10.20884/1.jm.2008.3.2.54
- Jing, P., Hou, M., Zhao, P., Tang, X., & Wan, H. (2013). Adsorption of 2-mercaptobenzothiazole from aqueous solution by organo-bentonite. *Journal of Environmental Sciences*, 25(6), 1139–1144. doi:10.1016/S1001-0742(12)60166-1
- Komadel, P. (2016). Acid activated clays: Materials in continuous demand. *Applied Clay Science*, 131, 84–99. doi:10.1016/j.clay.2016.05.001
- Kumararaja, P., Manjaiah, K. M., Datta, S. C., & Sarkar, B. (2017). Remediation of metal contaminated soil by aluminium pillared bentonite: Synthesis, characterisation, equilibrium study and plant growth experiment. *Applied Clay Science*, 137, 115–122. doi:10.1016/j.clay.2016.12.017
- Langmuir, I. (1918). THE ADSORPTION OF GASES ON PLANE SURFACES OF GLASS, MICA AND PLATINUM. *Journal of the American Chemical Society*, 40(9), 1361–1403. doi:10.1021/ja02242a004
- Lian, L., Guo, L., & Guo, C. (2009). Adsorption of Congo red from aqueous solutions onto Ca-bentonite. *Journal of Hazardous Materials*, 161(1), 126–131. doi:10.1016/j.jhazmat.2008.03.063
- Liu, Q.-S., Zheng, T., Wang, P., Jiang, J.-P., & Li, N. (2010). Adsorption isotherm, kinetic and mechanism studies of some substituted phenols on activated carbon fibers. *Chemical Engineering Journal*, 157(2–3), 348–356. doi:10.1016/j.cej.2009.11.013
- Maleki, A., Hayati, B., Najafi, F., Gharibi, F., & Joo, S. W. (2016). Heavy metal adsorption from industrial wastewater by PAMAM/TiO<sub>2</sub> nanohybrid: Preparation, characterization and adsorption studies. *Journal of Molecular Liquids*, 224, 95–104. doi:10.1016/j.molliq.2016.09.060
- Marsal, A., Bautista, E., Ribosa, I., Pons, R., & García, M. T. (2009). Adsorption of polyphenols in wastewater by organo-bentonites. *Applied Clay Science*, 44(1–2), 151–155. doi:10.1016/j.clay.2009.01.009
- Mishra, T., & Mahato, D. K. (2016). A comparative study on enhanced arsenic(V) and arsenic(III) removal by iron oxide and manganese oxide pillared clays from ground water. *Journal of Environmental Chemical Engineering*, 4(1), 1224–1230. doi:10.1016/j.jece.2016.01.022
- Önal, M., & Sarikaya, Y. (2007). Preparation and characterization of acid-activated bentonite powders. *Powder Technology*, 172(1), 14–18. doi:10.1016/j.powtec.2006.10.034
- Özcan, A. S., & Özcan, A. (2004). Adsorption of acid dyes from aqueous solutions onto acid-activated bentonite. *Journal of Colloid and Interface Science*, 276(1), 39–46. doi:10.1016/j.jcis.2004.03.043
- Parolo, M. E., Pettinari, G. R., Musso, T. B., Sánchez-Izquierdo, M. P., & Fernández, L. G. (2014). Characterization of organo-modified bentonite sorbents: The effect of modification conditions on adsorption performance. *Applied Surface Science*, 320, 356–363. doi:10.1016/j.apsusc.2014.09.105
- Pawar, R. R., Bajaj, H. C., & Lee, S. (2016). Activated bentonite as a low-cost adsorbent for the removal of Cu (II) and Pb (II) from aqueous solutions: Batch and column studies. *J. Ind. Eng. Chem*, 34, 213–223. doi:10.1016/j.jiec.2015.11.014

- Peng, X., Luan, Z., Chen, F., Tian, B., & Jia, Z. (2005). Adsorption of humic acid onto pillared bentonite. *Desalination*, 174(2), 135–143. doi:10.1016/j.desal.2004.09.007
- Rafatullah, M., Sulaiman, O., Hashim, R., & Ahmad, A. (2010). Adsorption of methylene blue on low-cost adsorbents: A review. *Journal of Hazardous Materials*, 177(1–3), 70–80. doi:10.1016/j.jhazmat.2009.12.047
- Redlich, O., & Peterson, D. L. (1959). A Useful Adsorption Isotherm. *The Journal of Physical Chemistry*, 63(6), 1024–1024. doi:10.1021/j150576a611
- Rostami, M. R., Kaya, M., Gür, B., Onganer, Y., & Meral, K. (2015). Photophysical and adsorption properties of pyronin B in natural bentonite clay dispersion. *Applied Surface Science*, 359, 897–904. doi:10.1016/j.apsusc.2015.10.079
- Shu, J., Wang, Z., Huang, Y., Huang, N., Ren, C., & Zhang, W. (2015). Adsorption removal of Congo red from aqueous solution by polyhedral Cu<sub>2</sub>O nanoparticles: Kinetics, isotherms, thermodynamics and mechanism analysis. *Journal of Alloys and Compounds*, 633, 338–346. doi:10.1016/j.jallcom.2015.02.048
- Slimani, R., El Ouahabi, I., Abidi, F., El Haddad, M., Regti, A., Laamari, M. R., ... Lazar, S. (2014). Calcined eggshells as a new biosorbent to remove basic dye from aqueous solutions: Thermodynamics, kinetics, isotherms and error analysis. *Journal of the Taiwan Institute of Chemical Engineers*, 45(4), 1578–1587. doi:10.1016/j.jtice.2013.10.009
- Taher, T., Mohadi, R., Rohendi, D., & Lesbani, A. (2017). Kinetic and thermodynamic adsorption studies of congo red on bentonite, in: AIP Conference Proceedings. AIP Publishing LLC, p. 020028. doi:10.1063/1.4978101
- Tomul, F. (2011). Synthesis, characterization, and adsorption properties of Fe/Cr-pillared bentonites. *Industrial & Engineering Chemistry Research*, 50(12), 7228–7240. doi:10.1021/ie102073v
- Toor, M., Jin, B., Dai, S., & Vimonses, V. (2015). Activating natural bentonite as a cost-effective adsorbent for removal of Congo-red in wastewater. *Journal of Industrial & Engineering Chemistry*, 21, 653–661. doi:10.1016/j.jiec.2014.03.033
- Wang, F., Pan, Y., Cai, P., Guo, T., & Xiao, H. (2017). Single and binary adsorption of heavy metal ions from aqueous solutions using sugarcane cellulose-based adsorbent. *Bioresource Technology*, 241, 482–490. doi:10.1016/j.biortech.2017.05.162
- Wang, L., & Wang, A. (2008). Adsorption properties of Congo Red from aqueous solution onto surfactant-modified montmorillonite. *Journal of Hazardous Materials*, 160(1), 173–180. doi:10.1016/j.jhazmat.2008.02.104
- Wang, W., Zheng, B., Deng, Z., Feng, Z., & Fu, L. (2013). Kinetics and equilibriums for adsorption of poly(vinyl alcohol) from aqueous solution onto natural bentonite. *Chemical Engineering Journal*, 214, 343–354. doi:10.1016/j.cej.2012.10.070
- Wang, Y., Xie, Y., Zhang, Y., Tang, S., Guo, C., Wu, J., & Lau, R. (2016). Anionic and cationic dyes adsorption on porous poly-melamine-formaldehyde polymer. *Chemical Engineering Research and Design*, 114, 258–267. doi:10.1016/j.cherd.2016.08.027
- Wasti, A., & Ali Awan, M. (2016). Adsorption of textile dye onto modified immobilized activated alumina. *Journal of the Association of Arab Universities for Basic and Applied Science*, 20, 26–31. doi:10.1016/j.jaubas.2014.10.001
- Xiyili, H., Çetintaş, S., & Bingöl, D. (2017). Removal of some heavy metals onto mechanically activated fly ash: Modeling approach for optimization, isotherms, kinetics and thermodynamics. *Process Safety and Environmental Protection*, 109, 288–300.

# Congo red dye removal from aqueous solution by acid-activated bentonite from sarolangun: kinetic, equilibrium, and thermodynamic studies

## ORIGINALITY REPORT

**20%**  
SIMILARITY INDEX

**20%**  
INTERNET SOURCES

**14%**  
PUBLICATIONS

**8%**  
STUDENT PAPERS

## PRIMARY SOURCES

<b>1</b>	<b>jaer.nuaca.am</b> Internet Source	<b>6%</b>
<b>2</b>	<b>mafiadoc.com</b> Internet Source	<b>2%</b>
<b>3</b>	<b>Submitted to Rutgers University, New Brunswick</b> Student Paper	<b>2%</b>
<b>4</b>	<b>www.semanticscholar.org</b> Internet Source	<b>1%</b>
<b>5</b>	<b>dns2.asia.edu.tw</b> Internet Source	<b>1%</b>
<b>6</b>	<b>Yi, Qingping, Ruiyi Fan, Feng Xie, Huiyu Min, Qinglin Zhang, and Zhengrong Luo. "Selective Recovery of Au(III) and Pd(II) from Waste PCBs Using Ethylenediamine Modified Persimmon Tannin Adsorbent", Procedia Environmental Sciences, 2016.</b> Publication	<b>1%</b>

7	<a href="http://www.karyailmiah.trisakti.ac.id">www.karyailmiah.trisakti.ac.id</a> Internet Source	1 %
8	<a href="http://www.thaiscience.info">www.thaiscience.info</a> Internet Source	1 %
9	I. Putu Mahendra, Adri Huda, Ha Minh Ngoc, Phan Trung Nghia, Tamrin Tamrin, Basuki Wirjosentono. " Investigation of TiO doped with nitrogen and vanadium using hydrothermal/Sol-Gel method and its application for dyes photodegradation ", Arab Journal of Basic and Applied Sciences, 2019 Publication	1 %
10	Ali Maged, Jibran Iqbal, Sherif Kharbish, Ismael Sayed Ismael, Amit Bhatnagar. "Tuning tetracycline removal from aqueous solution onto activated 2:1 layered clay mineral: Characterization, sorption and mechanistic studies", Journal of Hazardous Materials, 2020 Publication	1 %
11	Tarmizi Taher, Neza Rahayu Palapa, Risfidian Mohadi, Aldes Lesbani. "Adsorption behavior of Cr (VI) from aqueous solution by Fe-pillared acid activated Indonesian bentonite", AIP Publishing, 2019 Publication	1 %
12	<a href="http://hdl.handle.net">hdl.handle.net</a> Internet Source	1 %



13

Tarmizi Taher, Riza Antini, Lavini Indwi Saputri, Afifah Rahma Dian, Muhammad Said, Aldes Lesbani. "Removal of Congo red and Rhodamine B dyes from aqueous solution by raw Sarolangun bentonite: Kinetics, equilibrium and thermodynamic studies", AIP Publishing, 2018

Publication

1 %

14

Fatma Tomul. "Synthesis, Characterization, and Adsorption Properties of Fe/Cr-Pillared Bentonites", Industrial & Engineering Chemistry Research, 2011

Publication

1 %

15

Tarmizi Taher, Risfidian Mohadi, Aldes Lesbani. "EFFECT OF Ti<sup>4+</sup>/CLAY RATIO ON THE PROPERTIES OF TITANIUM PILLARED BENTONITE AND ITS APPLICATION FOR Cr (VI) REMOVAL", Rasayan Journal of Chemistry, 2018

Publication

1 %

16

Submitted to University of Aberdeen

Student Paper

1 %

Exclude quotes On

Exclude matches &lt; 1%

Exclude bibliography On